Nerve Microstructure: Modeling of the Diffusion MR Signal in Calibrated Model Systems and Nerves

Darya Morozov[1], Leah Bar[2], Nir Sochen[2], and Yoram Cohen[1]

[1]*School of Chemistry, Tel Aviv University, Tel Aviv, Israel,* [2]*School of Mathematical Sciences, Tel Aviv University, Tel Aviv, Israel*

Introduction: Diffusion tensor MR imaging (DTI), which assumes that water diffusion is Gaussian in neuronal tissues, is now routinely used for studying brain pathologies, connectivity and microstructure [1,2]. However at sufficient high diffusion weighting and long diffusion times, water diffusion in neuronal tissues is not Gaussian and effects of restricted diffusion can be observed. One way to analyze such diffusion data is by using the q-space approach first described by Callaghan [3,4], according to which when the signal intensity (E(**q**)) is plotted against the wave-vector **q** diffusion-diffraction minima, which reflect the size of the compartment, should be observed [3,4]. However, such diffusion-diffractions are not observed in many systems characterized by size polydispersity such as neuronal tissues. In such systems it was shown that the displacement distribution profile can be obtained after Fourier transform of the signal decay vs.**q** value [5]. This approach, which is in fact a non-parametric model free approach, was used to study restricted diffusion in neuronal tissues [6]. An alternative approach is to model the system by incorporating geometrical and other characteristics of the tissue and evaluate their effects on the signal decay. Such an early attempt was described by Stanisz et al., who constructed a three-pool model [7]. Assaf's CHARMED and Ax-Caliber models are also such parametrical models which are gaining more importance in recent years [8,9]. Recently, Alexander's group has developed and tested a series of possible models for diffusion in the CNS [10]. However, when models of increasing complexity are suggested we believe that is necessary to test them on real complex samples were the ground truth is known a priori. Such tests may allow one to evaluate the accuracy, the limitations and the performance of the suggested models prior to their use for studying complex neuronal tissues.

Objectives: To experimentally test a new model for studying diffusion using phantoms of increasing complexity in which the ground truth is known a priori. Subsequently to use this model to fit the signal decay in diffusion NMR experiments performed on fixed pig optic nerves.

Methods: Single-pulsed-field-gradient (s-PFG) experiments were performed in the x direction on a Bruker 8.4 T NMR spectrometer equipped with Micro5 probe capable of producing pulsed gradients of up to 190 G/cm in x-, y- and z- directions. Microcapillaries with known inner diameters (ID) of 5 ± 1, 9 ± 1, 15 ± 1 and 23 ± 1 and mixtures thereof were used both in the absence or presence of different amount of free diffusing water. For the microcapillaries of 23 ± 1 μm and a mixture of 23±1 and 14±1 μm (1:1 volumetric ratio) microcapillaries the PGSTE experiments were performed with δ of 2 ms and G_{max} of 160 G/cm, resulting in a maximal q value of 1362 cm^{-1}. Δ was set to 150 ms and the TE was 14 ms. For the mixture of 9±1 and 5±1 μm (1:1 volumetric ratio) microcapillaries the PGSTE experiments were collected with Δ= 50 ms, δ= 2 ms and 4 ms and G_{max} of 160 G/cm, yielding a maximal q value of 1362 and 2724 cm^{-1}, respectively and the TE was set to 32 ms. The fixed pig optic nerves, that were placed in a 8 mm NMR tube filled with Fluorinert, were studied when Δ was set to 30 or 90 ms, δ was 4 ms and G_{max} of 160 G/cm, yielding a maximal q value of 2724 cm^{-1}. This model is trying to fit the signal decay by a superposition of free Gaussian diffusion and a series of restricted diffusion in cylindrical geometries. No assumption is made on the number of compartments and only a size range has to be inserted a priori.

Results and Discussion: Figure 1A-C show the signal decay, along with the fitting of the experimental data, for PGSTE experiments performed on 23 ± 1 μm microcapillaries, a mixture of 23±1 and 14±1 μm microcapillaries and a mixture of 9±1 and 5±1 μm microcapillaries with increasing amounts of free diffusing water. The numerical values obtained from the fitting procedure are presented in Table 1. Only in the case of a single sized phantom clear diffusion-diffractions are observed, from which accurate size can be extracted. However, in all the samples our model, which looks for different modes of diffusion, can, even without prior knowledge on the number of components, identify the number of compartments, their diffusion mode as well as the size and fractions of the compartments where restricted diffusion occurs. The model also can identify the compartment in which Gaussian diffusion prevails. The fitting model requires only that the range of sizes will be inserted. Clearly the sizes that were extracted by fitting the experiment of data even for the three compartmental phantoms are very robust. Moreover the fitting was able to detect the correct number of restricted compartments and their fractions and to detect the increase in the fraction of free diffusing water in the sample. After challenging our model with samples where the ground truth is known, we decided to use it to obtain microstructural information on excised optic nerves. The fittings of data presented in Figure 1D were obtained while assuming diameters in the range of 0.6 to 12 μm.The numerical values for the fitting of the experiments performed with Δ of 30 or 90 ms and with δ of 4 ms, are tabulated in Table 1. We found that the results obtained from the two nerves are almost identical under the same experimental conditions. Clearly when δ was set to 4 ms and Δ was set to 30 ms or 90 ms, the could extract two mean axonal populations having diameters in the range of 2.6-2.7 μm and 5.4-5.7 μm for both optic nerves. We also found that higher diffusion weighting allows one to probe smaller compartments and increasing the diffusion time allows one to probe restriction in larger compartments. Longer diffusion times also allow for better differentiation between different compartments having different sizes.

Conclusions: We could demonstrate that our modeling is able, without assuming the number of compartments, to identify the number of restricted compartments, detect their sizes and determine their relative populations. The model is also able to identify and characterize free diffusion when presents in addition to the restricted compartments thus providing a suitable model for obtaining accurate microstructural information in neuronal tissues from diffusion experiments.

Figure 1. Signal decay in PGSTE experiments performed on phantoms of increasing complexity (A-C) and on optic nerves (D). Symbols indicate experimental data and the solid lines represent the fitting curves.

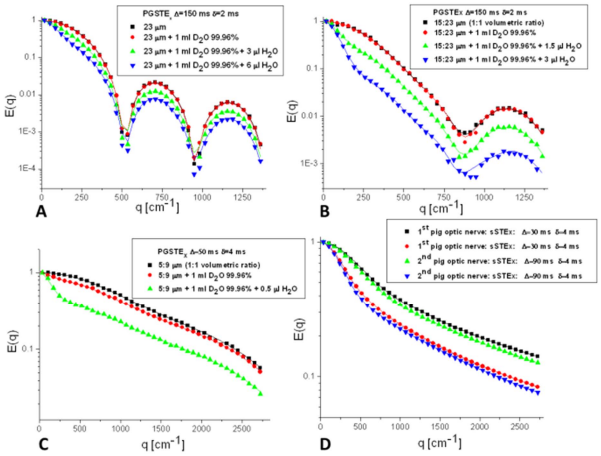

Table 1. Compartment sizes and volume fractions of the phantoms and optic nerve as obtained from modeling the PGSTE experiments.

system	free water	ID [μm]	restricted diffusion fraction	free diffusion fraction	standard deviation
23 μm	1ml D_2O	23.7	0.95	0.05	0.0069
	1 ml D_2O + 3 μl H_2O	23.8	0.58	0.42	0.0033
	1ml D_2O + 6 μl H_2O	23.7	0.35	0.65	0.0057
15:23μm	1ml D_2O	15.2 23.8	0.45 0.52	0.03	0.0078
	1 ml D_2O + 1.5 μl H_2O	15.2 23.6	0.19 0.19	0.62	0.0022
	1ml D_2O + 3 μl H_2O	15.2 23.4	0.06 0.06	0.88	0.0015
5:9 μm	1ml D_2O	5.2 9.0	0.43 0.41	0.16	0.0053
	1 ml D_2O + 0.5 μl H_2O	5.2 8.8	0.23 0.17	0.60	0.0074
optic nerve	a	2.7 5.7	0.277 0.203	0.520	0.0058
	b	2.6 5.4 8.6 12.0	0.16 0.15 0.09 0.12	0.48	0.0019

a). δ = 4 ms, Δ= 30 ms; **b).** δ = 4 ms, Δ= 90 ms

References: [1] D.K. Jones (Ed), Oxford University Press Inc., 2010. [2] H. Johansen-Berg , T.E.J. Behrens (Eds), Elsevier, Academic Press, 2009. [3] P.T. Callaghan et al., J. Magn. Reson., 90, 177-182 (1990). [4] P.T. Callaghan et al., Nature, 351, 467-469 (1991). [5] D.G. Cory, A.N. Garroway, Magn. Reson. Med., 14, 330-346 (1990). [6] Y. Cohen, Y. Assaf, NMR in Biomed., 15, 516-542 (2002). [7] G.J. Stanisz et al., Magn. Reson. Med., 37, 103-111 (1997). [8] Y. Assaf , P.J. Basser, Neuroimage, 27, 48-58 (2005). [9] Y. Assaf et al., Magn. Reson. Med., 59, 1347-1354 (2008). [10] E. Panagiotaki et al., NeuroImage, 59, 2241-2254 (2012).